Multivalent Nanoparticle Networks Enable Point-of-Care Detection of Human Phospholipase-A2 in Serum

Robert Chapman,[†,§] Yiyang Lin,[†,§] Mark Burnapp,[‡] Andrew Bentham,[‡] David Hillier,[∥] Abigail Zabron,[∥] Shahid Khan,[∥] Matthew Tyreman,[‡] and Molly M. Stevens*[,†]

[†]Department of Materials, Department of Bioengineering and Institute for Biomedical Engineering, Imperial College London, London SW7 2AZ, U.K., [‡]Mologic Ltd., Bedford Technology Park, Thurleigh, Bedfordshire MK44 2YP, U.K., and [∥]Hepatology and Gastroenterology Section, Faculty of Medicine, St Mary's Hospital Campus, Imperial College London, London W2 1NY, U.K. [§]R. Chapman and Y. Lin contributed equally.

ABSTRACT A rapid and highly sensitive point-of-care (PoC) lateral flow assay for phospholipase A_2 (PLA_2) is demonstrated in serum through the enzyme-triggered release of a new class of biotinylated multiarmed polymers from a liposome substrate. Signal from the enzyme activity is generated by the adhesion of poly-streptavidin-coated gold nanoparticle networks to the lateral flow device, which leads to the appearance of a red test line due to the localized surface plasmon resonance effect of the gold. The use of a liposome as the enzyme substrate and multivalent linkers to link the nanoparticles leads to amplification of the signal, as the cleavage of a small amount of lipids is able to release a large amount of polymer linker and adhesion of an even larger amount of gold nanoparticles. By optimizing the molecular weight and multivalency of these biotinylated polymer linkers, the sensitivity of the device can be tuned to enable naked-eye detection of 1 nM human PLA_2 in serum within 10 min. This high sensitivity enabled the correct diagnosis of pancreatitis in diseased clinical samples against a set of healthy controls using PLA_2 activity in a point-of-care device for the first time.

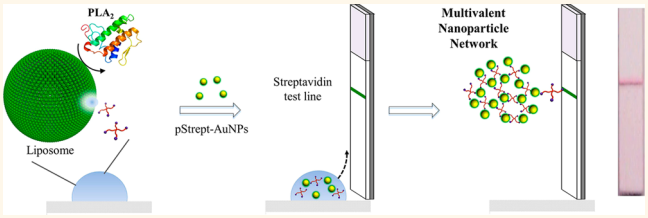

KEYWORDS: multivalent network · point of care · phospholipase · biosensor · lateral flow device

Phospholipases A2 (PLA_2) are a subfamily of phospholipase that catalyze the hydrolysis of the *sn*-2 fatty acyl chain of phospholipids to yield a fatty acid and a lysophospholipid.[1,2] PLA_2 could be a potential marker for diagnosing diseases including atherosclerosis,[3] pancreatitis,[4] acute sepsis,[5] prostate cancer,[6,7] and lung cancer.[8] The sensitivity of commercial assay kits for measurement of PLA_2 activity is well below the levels required for clinical diagnosis (see Supporting Information). Although many sensitive assays have been developed,[9−12] they typically use the more active venom forms of the enzyme in simple buffers, and a point-of-care assay sensitive enough to detect human phospholipase A2 activity at clinically relevant levels in serum is not available.

Lateral flow testing has become the standard bioassay format for point-of-care diagnostic assays because these assays are rapid, easy-to-use, portable, disposable, and low-cost. The strip platform can detect clinically relevant analytes without highly qualified personnel, complicated data analysis, or expensive equipment. The diagnostic result can be obtained visually from the color intensity of signals on the test line. The utilization of modern imaging devices (*e.g.*, cameras and smart phones) to capture and analyze the colorimetric signals and transmit the data off-site enables a long-distance diagnostic of patient health.[13,14] Recently, lateral flow assays of nucleic acids,[15] RNA,[16] proteins,[17] cancer cells,[18] metal ions,[19] and small molecules[20] have been reported. Despite this, most examples of these assays are affinity-based antibody tests or small-molecule tests. The detection of human phospholipase A2 activity on a lateral flow device has not been reported.

To develop a point-of-care sensor of human PLA_2 activity, a lateral flow device was designed by coupling gold nanotechnology and multivalent interactions. Gold nanoparticles (AuNPs) possess distinct physical and chemical attributes that make them excellent

* Address correspondence to m.stevens@imperial.ac.uk.

Received for review October 9, 2014 and accepted February 27, 2015.

Published online March 10, 2015
10.1021/nn5057595

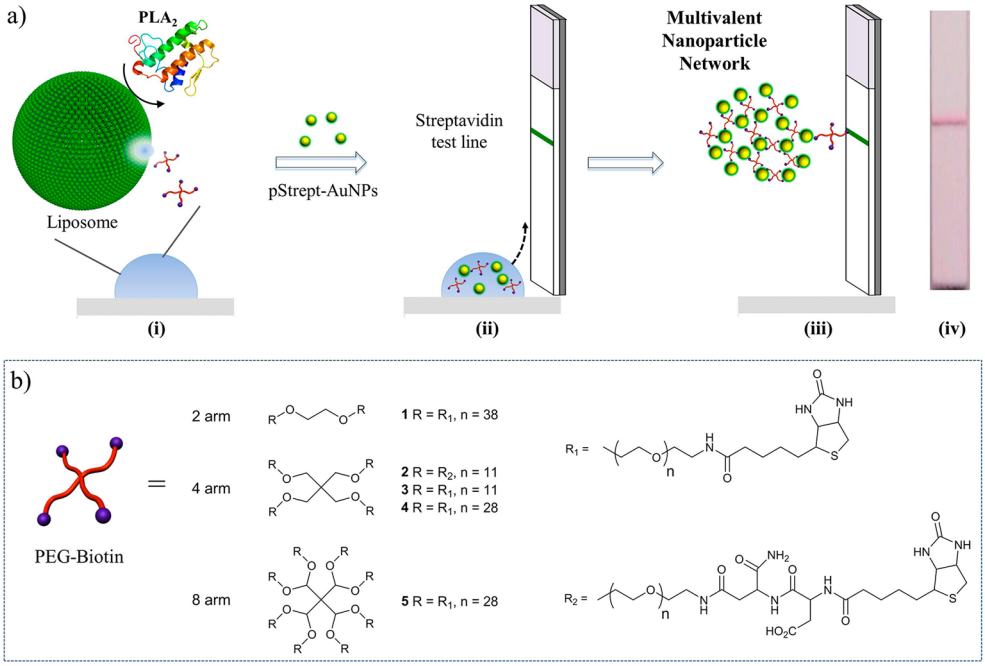

Figure 1. (a) Lateral flow assay schematic. (i) Biotinylated PEG linkers loaded liposomes are incubated with PLA_2, which cleaves liposome and releases PEG linker. (ii) Polystreptavidin-coated gold nanoparticles (pStrept-AuNPs) are then mixed with the liposome/PLA_2 solution, introduced to a lateral flow strip, and run up the nitrocellulose membrane by capillary forces. A test line on the strip is preprinted with streptavidin as indicated by the green line. (iii) If the liposome is cleaved, the linker will adhere pStrept-AuNPs to the test line by forming multivalent nanoparticle networks. (iv) A representative lateral flow strip with a signal from bound AuNPs is shown. (b) Structures of biotinylated PEG linkers 1−5 investigated.

candidates for designing biological sensors.[21−24] Nanosized gold provides a high surface-to-volume ratio with excellent biocompatibility, enabling surfaces functionalized with biological ligands such as peptides, DNA, and proteins. AuNPs possess unique optoelectronic properties (*e.g.*, surface plasmon resonance and surface enhanced Raman scattering) that are dependent on the size, shape, and the surrounding chemical environment.[24] For example, AuNPs show a much higher molar extinction coefficient (ε) (7.66×10^9 M^{-1} cm^{-1} at 528 nm for 40 nm AuNPs) than common organic dyes, such as rhodamine 6G ($\varepsilon = 1.16 \times 10^5$ M^{-1} cm^{-1} at 530 nm). The aggregation/disaggregation of AuNPs induces interparticle surface plasmon coupling, resulting in a visible color change at nanomolar concentrations, which provides a practical platform for colorimetric sensing of target analytes.[21−27] Based on four-helix heteroassociation of peptide interaction induced AuNP aggregation, a sensitive assay for snake venom phospholipase ($vPLA_2$) was developed in our previous work.[28,29]

Multivalency, as characterized by simultaneous binding of multiple ligands on multiple receptors, is prevalent and essential in biological recognition events.[30−33] Modulating the valency of the interactions between gold nanoparticles is expected to significantly enhance the interparticle interactions and hence increase the sensitivity of nanoparticle-based bioassays.[34] In this work we demonstrate the design of a class of biotin-conjugated multiarm PEG linkers and employ them to fabricate a highly sensitive lateral flow device for the point-of-care detection of phospholipase A2 in serum.

RESULTS AND DISCUSSION

A schematic of the assay design is shown in Figure 1a. In the first step, enzymatic cleavage of phospholipids by phospholipase A2 causes the release of biotinylated multiarm PEG linkers from a liposome. This solution is then mixed with polystreptavidin-coated AuNPs (pStrept-AuNPs) and driven by capillary forces to flow up a nitrocellulose membrane. The poly(ethylene glycol) (PEG) linkers adhere the pStrept-AuNPs to a test line of streptavidin *via* biotin−streptavidin affinity, and the signal can be read with the naked eye due to the localized surface plasmon resonance (LSPR) effect of the AuNPs. If no enzyme (and thus no linker) is present, the pStrept-AuNPs should flow past the test line without adhering. The assay employs two signal amplification mechanisms. the first amplification coming from the release of multiple PEG linkers from a single liposome and the second coming from the network of gold nanoparticles that can form on the test line through multivalent interactions. Because the signal is generated by biotin−streptavidin interactions, the device should work very sensitively even in high concentrations of serum.

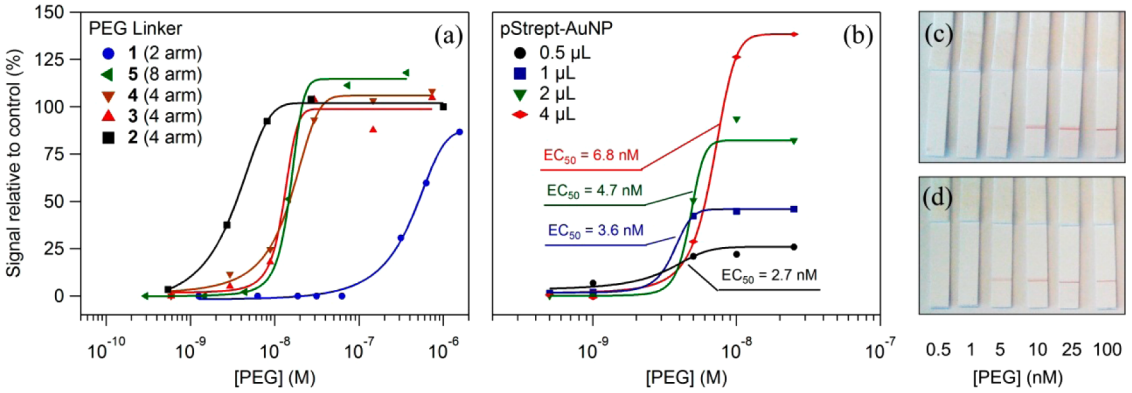

Figure 2. Comparison of linker sensitivity as measured on lateral flow strips in 10 mg/mL BSA in PBS. Signal strength *vs* PEG concentration is shown (a) for all five linkers with 2 μL of pStrept-Au and (b) for linker 2 with 0.5, 1, 2, and 4 μL of pStrept-Au. Sigmoidal fits for each data set are shown. (c, d) Example photographs of the test strips after being run with linker 2 and (c) 4 μL and (d) 2 μL of pStrept-Au.

Development of PEG Linkers. A variety of multiarm PEG linkers (Figure 1b and Table S1) were synthesized by standard amide coupling of biotin to dendrimeric amine-terminated PEG molecules. Various molecular weights and dendrimer generations (2−8 arm molecules) were studied. The effect of charge was investigated by preparing Asp-Asp-Biotin *via* solid phase peptide synthesis (SPPS) on rink amide resin and then coupling this instead of biotin to the PEG. The biotin functionalization was confirmed by ^{1}H NMR (Supporting Information, Figure S1) and by a HABA/avidin assay. The efficiency of the linkers in forming multivalent nanoparticle networks was evaluated on nitrocellulose test strips (CN140) by measuring the amount of signal generated from the adhesion of 40 nm AuNPs coated with polystreptavidin to the test line. For each PEG linker the strength of the signal was plotted against PEG concentration and the data were fit to a sigmoidal curve (Figure 2a). A set of representative photographs of these test strips is shown in Figure 2c,d. The midpoint of this sigmoidal fit was used to evaluate the efficiency of biotinylated PEG to cross-link pStrept-AuNPs, expressed as an EC_{50}. The high intensity of the signal at optimum linker concentrations demonstrates the capability of PEG linkers to generate multivalent nanoparticle networks.

As shown in Figure 2a, linker **1** was the worst performing of the PEG linkers we investigated, requiring a concentration of more than 1 μM of PEG to generate a strong signal from the adhesion of pStrept-AuNPs to the test strip. This was unsurprising, as the linker had only two biotin functionalities per chain. In this case the chance of intraparticle binding of linker **1** would be expected to be relatively high. Even for interparticle binding, the monovalent affinity between two nanoparticles would not be expected to be as strong as in the case of the multiarm PEG systems. Increasing the number of biotin functionalities per PEG molecule was found to improve the sensitivity of the system markedly. Linkers **4** and **5**, prepared from the four- and eight-arm PEG molecules, respectively, both showed EC_{50}'s of approximately 20 nM, representing more than an order of magnitude improvement in sensitivity over the bifunctional linker **1**. The maximum signal intensity was also enhanced significantly by using these multiarm linkers, indicating the formation of stronger AuNPs networks. It is interesting that the four-arm (linker **4**) and eight-arm (linker **5**) dendrimers demonstrated similar sensitivity despite the presence of almost twice as much biotin per molecule in the case of the eight-arm dendrimer. This is likely because both PEG molecules, which we estimate to have a Flory radius of <5 nm,[35] are small relative to the 50 nm pStrept-AuNPs (Figure 3a). Because of this, once a PEG linker has cross-linked two or three pStrept-AuNPs even if free biotin groups remain, there should be no space for further nanoparticles to access them, explaining why increasing the number of arms above four had little effect on sensitivity. Similarly, the molecular weight of the PEG was also found to have little effect on sensitivity. As can be seen in Figure 2a, the four-arm PEG linkers with different molecular weights (linkers **3** and **4**) displayed very similar response curves. However, the inclusion of a negative charge onto the end of each PEG arm was found to dramatically improve sensitivity, as can be seen by comparing linkers **2** and **3**. Both of these linkers were prepared from the same PEG starting material, but linker **2**, which contained one carboxylic acid group per biotin, demonstrated almost three times higher sensitivity and stronger signal. We hypothesize that without this negative charge the hydrophobic nature of biotin causes some aggregation of the biotin groups in water, preventing the display of the groups on the surface of the PEG linker and reducing the efficiency with which it can cross-link the pStrept-AuNPs. The introduction of the negative charge would be expected to cause the molecule to swell to a larger hydrodynamic radius and more effectively cross-link two different

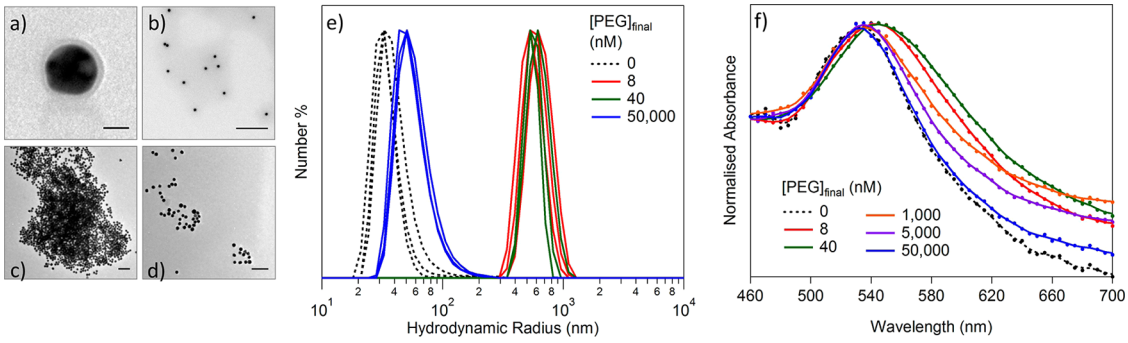

Figure 3. Aggregation of 40 nm pStrept-AuNPs with PEG linker 2 in PBS. TEM images of pStrept-AuNPs (a and b); with 40 nM (c); and with 5000 nM (d) of linker 2. Scale bar (a−d) = 20, 500, 200, and 200 nm, respectively. (e) UV/vis and (f) DLS spectra of AuNPs after 20 h incubation with linker 2.

nanoparticles as we observe experimentally. At very high concentrations of linker, approximately 30 μM PEG in the case of linker **2**, the signal from the binding of pStrept-AuNPs to the test strip is greatly reduced. Presumably, at this concentration the PEG linker is in such excess that it coats the gold entirely, using up all the available streptavidin sites and preventing the aggregation of the particles. The effect of gold concentration on the signal was also investigated (Figure 2b). Higher concentrations of pStrept-AuNPs resulted in stronger signal, but slightly decreased sensitivity. The EC_{50} of linker **2** was found to increase from 2.7 nM to 3.6, 4.7, and 6.8 nM as the volume of pStrept-AuNPs was increased from 0.5 μL to 1, 2, and 4 μL, respectively. At 4 μL of Strept-Au the background due to nonspecific adsorption of the particles on the strip below the test line is quite significant (Figure 2c), and so in order to retain a sensitive assay with a high signal intensity but low background, we chose to use 2 μL for all subsequent experiments.

The results from the test strip experiments were confirmed using UV/vis spectroscopy, dynamic light scattering (DLS), and transmission electron microscopy (TEM). As shown in Figure 3a and b, pStrept-AuNPs are well dispersed in solution, with the diameter of 40 nm and a uniform shell of ~5 nm. The shell thickness is close to the diameter of streptavidin (4 nm),[36] indicating a single-layer coating on AuNPs. At a linker **2** concentration of 8−40 nM, strong aggregation of the pStrept-AuNPs into a multivalent nanoparticle network was observed by TEM (Figure 3c), and the hydrodynamic diameter of the particles as measured by DLS (Figure 3e) increased from approximately 40 nm to almost 1000 nm in both cases. The UV/vis spectrum of the pStrept-AuNP solution (Figure 3f) shows a shift of only 10−15 nm, much less than other AuNP systems.[29] This is presumably due to the large distance between each AuNP inside the multivalent nanoparticle networks. In the case of networks from the four-arm PEG (2 kDa), for example, the extended length of each PEG chain would be ~6 nm, and the total distance between two AuNPs would be expected to be greater than 20 nm. This limits the extent of the LSPR peak shift after aggregation of the particles. As the concentration of linker was increased to 5 μM, the amount of aggregation was significantly reduced (TEM in Figure 3d) with a small SPR shift of <5 nm. The average hydrodynamic diameter from DLS was measured to be 100 nm, suggesting weak aggregation of AuNPs. These results support the results from the test strips at high linker concentrations.

Measurement of Human PLA_2 Activity in Serum. In order to test the sensitivity of the full assay, the activity of phospholipase A2 (*v*PLA_2, *Naja mossambica mossambica*) was measured against 1-palmitoyl-2-oleoyl-*sn*-glycero-3-phosphocholine (POPC) liposomes. As linker **2** was determined to be the most sensitive, unilamellar liposomes (~200 nm) loaded with this linker were prepared by an extrusion method and purified by gel filtration through a Sephadex G-100 column. TEM and DLS were used to confirm the narrow size distribution of the liposomes (see Supporting Information, Figures S3−S5). The liposomes, enzyme, and assay buffer containing 10 mg/mL BSA in PBS were mixed together in a droplet on Parafilm wax and incubated together at room temperature. After this incubation, pStrept-AuNPs were added and the mixture was introduced to the test strips. After 5 min, the strips were washed with a solution of BSA in PBS (10 mg/mL) to remove any unadhered AuNPs. The resulting signal was read using a commercial lateral flow device reader against a reference line from an assay run with 2 μL of Tween 20 (10 wt %). Increasing the concentration of linker loaded inside the liposome was found to improve the sensitivity of the assay toward *v*PLA_2 (Figure 4a), and optimum sensitivity was observed at 0.2 mM linker. Increasing the concentration of liposomes in the assay was found to have a limited effect on the sensitivity, presumably because at the lowest concentration tested (2 μL) the concentration of liposomes is far higher than the concentration of enzyme. Under these conditions the limit of detection was determined to be below 0.5 nM *v*PLA_2. Not only is this assay format significantly faster than the traditional

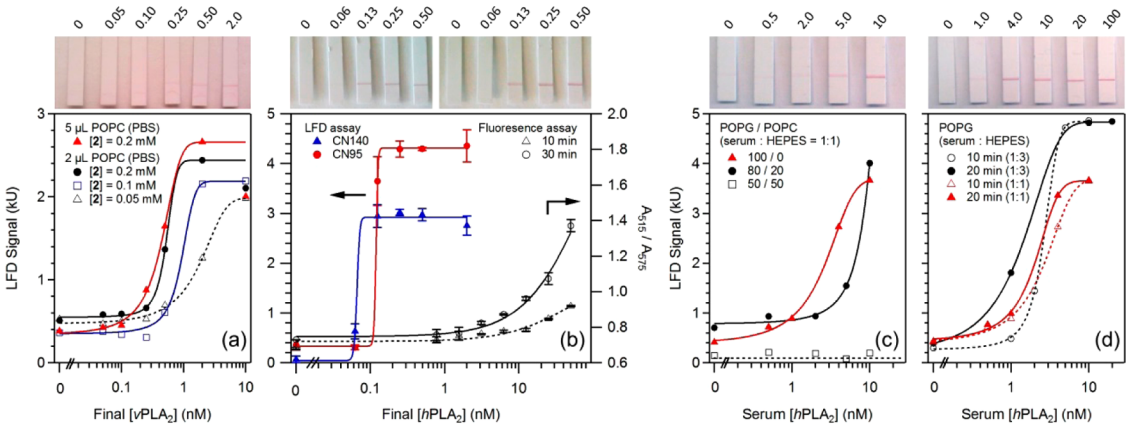

Figure 4. Sensitivity of the lateral flow assay to PLA_2 using liposomes loaded with linker 2. (a) POPC liposomes (2 or 5 μL) loaded with 0.05, 0.1, and 0.2 mM of linker against *v*PLA_2 in PBS assay buffer. Photographs of the 2 μL liposome loaded with 0.2 mM linker 2 are shown. (b) Comparison of the lateral flow device (LFD assay) on CN95 and CN140 membranes with the commercial life sciences fluorescence assay for detection of PLA2GIB activity. LFD assay was performed using POPG liposomes with a HEPES assay buffer. $n = 3$, SD shown in the error bar. Representative photographs of the test strips are shown for both the CN140 (left) and CN95 (right) series. (c) POPG/POPC (50/50, 80/20, and 100/0 w/w) liposomes against PLA2GIB in 1:1 serum/HEPES assay buffer. Photographs from the 80/20 POPG/POPC series are shown. (d) POPG liposomes against PLA2GIB in 1:3 (pictures shown) and 1:1 serum/HEPES assay buffer. All liposomes were incubated for 10 min with the enzyme before addition of pStrept-AuNPs unless otherwise indicated.

fluorescence-based assays, it is also approximately an order of magnitude more sensitive compared to the widely used carboxyfluorescein quenching method, which gives a detection limit of ~1.0 nM.[29] The liposomes were found to be very stable, and no increase in background signal due to the leakage of PEG linker was observed over 3 weeks (see Supporting Information, Figure S6). It is likely that long-term storage of liposomes for applications in commercial devices could be achieved by drying them in sugar glasses, and this is a subject of ongoing investigation.[37]

In order to establish clinical relevance, we wanted to translate the assay from the measurement of the activity of snake enzyme (*v*PLA_2) to the less active human form (*h*PLA_2). Here a recombinant form of human pancreatic phospholipase A_2 (PLA2GIB) was used, since it is a potential biomarker in serum for acute pancreatitis. It is reported that PLA2GIB binds to liposome membrane in the trimeric form through the back, positively charged surface.[12,38] Hence we hypothesized that PLA2GIB should be more active toward lipids with negatively charged head groups than toward neutral lipids such as POPC. To this end, negatively charged liposomes were prepared from either mixed POPC/POPG or pure POPG with the encapsulated linker **2**. The increased negative charge of these liposomes relative to the POPC liposomes was confirmed by zeta potential, which was observed to drop from −2.4 mV in the case of the POPC liposomes to −33.2 mV in the case of the POPG liposomes (see Supporting Information, Table S2). The *h*PLA2GIB was indeed found to be highly active toward pure POPG liposomes, and EC_{50}'s below final enzyme concentrations of 0.1 nM could be achieved in HEPES buffer. In Figure 4b, the POPG lateral flow assay is compared with a commercial Invitrogen assay for PLA_2. As with all existing commercial assays for PLA_2, this assay is based on the increase in Förster resonance energy transfer (FRET) signal from lipid cleavage and thus is not amenable to application at point of care. As can be seen, the point-of-care lateral flow device assay described here demonstrates a limit of detection at almost 2 orders of magnitude less *h*PLA2GIB than the commercial assay. Two different nitrocellulose membranes with different running speeds were compared (see Supporting Information, Table S3, for technical specifications). The faster running CN140 membrane was found to result in a slightly lower top signal than the slower CN95 membrane, but also gave a slightly lower EC_{50} value. As the top signal was strong in both cases and because the CN140 membrane enables a faster assay speed, this membrane was used in all subsequent experiments.

The POPC/POPG and pure POPG liposomes were found to be stable in 1:1 mixtures of HEPES buffer and serum, and this enabled the translation of the assay into clinically relevant media. In POPC/POPG (50/50 w/w) liposomes, no signal at up to 10 nM of *h*PLA2GIB in serum was observed, but as expected, as the ratio of POPG was increased, the sensitivity of the assay toward the enzyme improved (Figure 4c). The 100% POPG liposomes were found to be the most sensitive, and the limit of detection of *h*PLA2GIB in serum was determined to be 1 nM, in either 1:1 or 1:3 dilutions of serum:HEPES assay buffer (Figure 4c,d). No nonspecific binding of pStrept-AuNPs to the test line was observed even at this high concentration of serum. Such a limit of detection gives the assay excellent applicability for the clinically relevant range of 1−10 nM.[4,39] Slightly improved sensitivity was

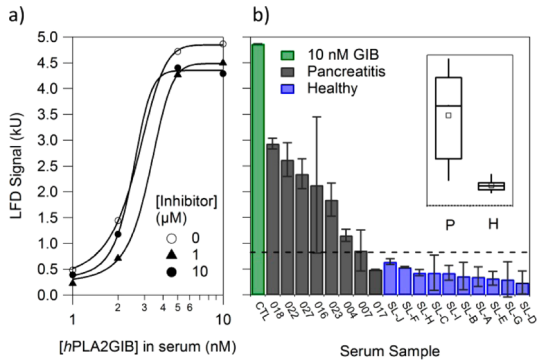

Figure 5. (a) LFD standard curves showing equal sensitivity toward *h*PLA2GIB at different concentrations of PLA2GIIA inhibitor. (b) LFD results from a 10 nM PLA2GIB control sample (CTL), 8 pancreatic sera samples (#018, #022, #027, #016, #023, #004, #007, and #017), and 10 healthy sera controls (SL A–J). Dotted line indicates a clearly visible signal. Inset: Box plots showing the 25th, median, and 75th percentile for the pancreatic (P, *n* = 8) and healthy (H, *n* = 10) samples. Whiskers are drawn showing the 10th and 90th percentile, and the open squares indicate the mean LFD signal in each set.

observed when the liposomes and enzyme were incubated for 20 min instead of 10 min before introduction of the AuNPs and the test strip, although the effect was marginal (Figure 4d).

Diagnosis of Acute Pancreatitis. Before moving on to the measurement of *h*PLA_2 in clinical samples to determine the suitability of the assay to diagnose acute pancreatitis, it was important to ensure that only the pancreatic form of PLA_2 would interact with the liposomes. Endogenous *h*PLA_2 can be found in two major forms in serum: group IB (PLA2GIB), which is known to be the pancreatic form of the enzyme and a good marker for acute pancreatitis, and group IIA (PLA2GIIA), which is an inflammatory enzyme that can be present for a variety of other reasons including sepsis,[40] rheumatoid arthritis,[41] and various cardiac conditions.[42,43] Because POPG liposomes were found to be equally sensitive to cleavage by both (Supporting Information, Figure S7), it was important to inhibit the PLA2GIIA form of the enzyme using the commercial inhibitor LY311727 before measuring the PLA2GIB activity in any clinical serum samples.[44] Incubation of enzyme with 10 μM of this inhibitor for 1–10 min in diluted serum was found to completely remove activity of up to 200 nM recombinant PLA2GIIA in control sera and endogenous PLA2GIIA from a range of healthy sera (Supporting Information, Figure S8). The specificity of the inhibitor toward the GIIA form of the enzyme was found to be extremely high, and despite completely removing all PLA2GIIA activity, the inhibitor was found to impart no loss in activity of 1–10 nM of the GIB form, even when no GIIA was present (Figure 5a).

To test the clinical relevance of the device, we used this assay format to measure the PLA2GIB activity in a series of sera samples from emergency room patients diagnosed with acute pancreatitis. Because the commercial activity kit could measure serum activity of only 50 nM PLA_2 (Figure 4b), it was not able to detect any activity in these sera. Therefore, a comparison of our assay to existing tests was not possible on these samples. All of the pancreatitis samples were collected within 24 h of admittance to the hospital and showed elevated levels of both amylase and lipase (Supporting Information, Figure S9), confirming the diagnosis. All samples were diluted (1:3) with assay buffer containing 10 μM of inhibitor and left for 10 min before addition of the liposomes. The signals generated by the samples from patients with pancreatitis were compared with the signals from a set of healthy control sera that were purchased through Seralabs. As can be seen from Figure 5b, all except one of the pancreatitis samples showed significantly stronger signals than any of the healthy control samples.

These results demonstrate the design of a point-of-care test with sufficient sensitivity and selectivity to detect the GIB form of human PLA_2 in the presence of the GIIA form in serum for the diagnosis of acute pancreatitis. The format of the assay makes it immediately applicable to the design of a commercial assay. We were able to show that the gold nanoparticles can be incorporated directly into the laminar flow strip rather than premixed with the serum and liposomes without loss of sensitivity toward *h*PLA2GIB (see Supporting Information, Figure S10). In addition we were able to show the incorporation of an internal control line by printing rabbit IgG above the test line and mixing AuNPs conjugated to a goat anti-rabbit antibody with the pStrept-AuNPs before running the assay (see Supporting Information, Figure S11). Both of these results demonstrate the assay to be highly robust and in a format that could be immediately applied to a commercial product and used at point of care.

CONCLUSIONS

A class of biotinylated multiarm PEG linkers was designed and exploited to trigger the aggregation of polystreptavidin-coated gold nanoparticles at high sensitivity. The formation of multivalent nanoparticle networks *via* multivalent interactions was demonstrated by TEM, DLS, UV/vis, and lateral flow strip test. The performance of PEG linkers could be significantly enhanced by increasing the number of PEG arms or introducing a charge group to biotin, owing to the enhanced multivalent interactions. A very sensitive lateral flow device for *h*PLA_2 (as distinct from the more active snake venom PLA_2) was designed by using four-arm PEG linkers, which was able to give a detection limit of 1 nM in serum and 0.1 nM in buffer. Such high sensitivity enabled the accurate diagnosis of acute pancreatitis in clinical samples using a point-of-care device. The assay can be completed within 20 min without complex analysis, expensive machine, or

highly trained personnel. The result of the lateral flow assay was captured and transduced by smart phone and could meet the criteria of a long-distance point-of-care diagnostic.

EXPERIMENTAL SECTION

Reagents. Phospholipase A2 from *Naja mossambica mossambica*, avidin, hydroxyazobenzene-2-carboxylic acid (HABA), bovine serum albumin (BSA), and human serum from human male AB plasma (control serum) were purchased from Sigma-Aldrich (UK) and used without further purification. Human sera (female only individual) were purchased from Sera Laboratories International Ltd. (UK). 1-Palmitoyl-2-oleoyl-*sn*-glycero-3-phosphocholine (POPC) and 1-palmitoyl-2-oleoyl-*sn*-glycero-3-phospho(1′-*rac*-glycerol) (POPG) were purchased from Avanti Polar Lipids (Alabaster, AL, USA). Phospholipase A2 inhibitor LY 311727 was purchased from Tocris Bioscience (UK). Recombinant human phospholipase A2 group IB/PLA2GIB and group IIA/PLA2GIIA were bought from R&D Systems. AuNP solution (40 nm) was from BBI Solutions. Multiarm PEG amines were bought from JenKem Technology (USA). Polystreptavidin and nitrocellulose membranes with a polystreptavidin test line were obtained from Alere (UK). The lateral flow strips, produced from CN140 and CN95 nitrocellulose membranes, were provided by Mologic Ltd. (UK). The strips were 25 mm long and 5 mm wide. The distance between the test line and the bottom of the strip was 7 mm.

To prepare polystreptavidin-coated AuNPs, polystreptavidin (1 mg/mL, 50 μL) was added to a suspension of citrate-stabilized 40 nm gold nanoparticles in 20 mM borate buffer (pH 9.3). After 30 min, 100 μL of BSA (20 mg/mL) was added, and the suspension was left overnight at 4 °C. The nanoparticles were purified by centrifugation at 4000*g* and subsequent replacement of the supernatant four times with borate buffer.

Synthesis of Biotin-Functionalized PEG Linkers. Biotinylated PEGs were synthesized by direct coupling of biotin or Asp-Asp-biotin to PEG using the 1-ethyl-3-[3-(dimethylamino) propyl]carbodiimide hydrochloride (EDC)/*N*-hydroxysuccinimide (NHS) method. Typically, four-arm PEG (0.1 mmol, 200 mg), EDC (1.0 mmol, 192 mg), NHS (0.5 mmol, 58 mg), and biotin (1.0 mmol, 224 mg) were added in DMSO and stirred for 48 h. The product was applied to dialysis against water using dialysis tubing (MWCO 1000).

HABA/Avidin Assay. Quantification of biotin was conducted using HABA/avidin reagent. Briefly, the HABA/avidin reagent was prepared according to the manufacturer's instructions by adding 10 mg of avidin and 600 μL of HABA solution (24.2 mg in 9.9 mL of water and 0.1 mL of 1 M NaOH) to 19.4 mL of PBS. The absorbance before and after addition of 20 μL of PEG linker in water to 180 μL of the HABA/avidin solution was measured at 500 nm using a UV/vis spectrometer. The concentration of biotin was determined from the quenching of the HABA absorbance by biotin, using the Beer–Lambert law (where ε = 34 500 M^{-1} cm^{-1}, and l = 1 cm).

$$[\text{Biotin}] = (\text{Abs}_{\text{initial}}(180/200) - \text{Abs}_{\text{final}})/\varepsilon$$

Liposome Preparation and Characterization. PEG linkers-loaded unilamellar liposomes were prepared by extrusion through a 200 nm membrane. In detail, the lipid solution in chloroform was first dried under a stream of nitrogen, then placed under vacuum for at least 2 h to remove any residual solvent. The dried lipid film containing 5 mg of lipid was then rehydrated in 1 mL of 0.2 mM PEG linkers in buffer solution and vortexed. The resulting solution was extruded 19 times through a polycarbonate membrane with 200 nm pores (Nucleopore). Untrapped PEG linkers were removed from the liposome suspension by gel filtration through a Sephadex G-100 column (20 cm × 0.5 cm). The liposome solution was diluted to 1.0 mg/mL of lipid concentration, stored at 4 °C, and used within 2 weeks.

Transmission electron microscopy was performed on a JEOL 2000FX (working voltage of 200 kV) by a negative-staining method with 1.0 wt % uranyl acetate solution as the staining agent. Dynamic light scattering and zeta potential were measured on a Malvern Zetasizer Nano ZS (Malvern, UK).

Analytical Procedure. To evaluate the performance of different PEG linkers, 2 μL of polystreptavidin-coated Au nanoparticles were mixed with PEG linkers in PBS buffer containing 5 mg/mL BSA on a piece of Parafilm wax. The mixture was applied to CN140 lateral flow strips, and the strips were washed with a solution of BSA in PBS (10 mg/mL) to remove nonspecific binding Au nanoparticles.

For lateral flow assays against *v*PLA_2, 0.2 mM linker **2** was incorporated in POPC liposomes with the final lipid concentration of 1 mg/mL. On a piece of Parafilm wax, 2 or 5 μL of liposome solution was incubated with *v*PLA_2 in 20 μL of PBS assay buffer containing $CaCl_2$ (2 mM) and BSA (10 mg/mL) for 10 min at room temperature. A 2 μL amount of pStrept-AuNPs was then added, and the mixture was introduced to the CN140 test strips. Capillary forces drive the solution to run up the strips within 2 min. The strips were then washed with a solution of BSA in PBS (20 mg/mL) to remove any unadhered gold. For assays against *h*PLA_2, 0.2 mM linker **2** in HEPES (50 mM)/NaCl (150 mM) was incorporated in POPG or POPC/POPG (20/80 or 50/50 w/w) liposomes and diluted to a final lipid concentration of 1 mg/mL after purification. A 5 μL portion of liposomes was mixed with 20 μL of serum diluted in assay buffer containing HEPES (50 mM), $CaCl_2$ (20 mM), NaCl (150 mM), and BSA (10 mg/mL) and incubated with the enzyme before addition of 2 μL of pStrept-AuNPs as above. After this the solution was introduced to the test strips and washed with 20 μL of HEPES assay buffer. In all cases the signal on the test line was recorded using a commercial lateral flow device reader from Forsite Diagnostics (LFDR101). The test line was measured relative to a reference line, which was created by running a strip with 5 μL of POPG, 20 μL of HEPES assay buffer, 2 μL of pStrept-AuNPs, and 2 μL of Tween 20 (10 wt %). Lateral flow devices with AuNPs predried on the strip were prepared by drying 4 μL of pStrept-AuNPs on a glass fiber pad, which was adhered to the bottom of the test strip. These devices were run as above, but were washed with 55 μL instead of 20 μL of assay buffer.

Internal Control Line Experiments. Test strips were prepared on CN140 nitrocellulose membranes with a polystreptavidin test line as above and with a control line of rabbit IgG. Both were printed from a 1 mg/mL solution in PBS. A goat anti-rabbit gold conjugate using the same method as for the pStrept-AuNPs and both populations of nanoparticles were mixed prior to running the devices as above.

Clinical Sample Collection. Clinical pancreatitis samples were collected at Hammersmith Hospital, London, UK, between March and May 2013. Informed written consent was obtained in each case, under approval by the local ethics committee (REC reference 09/H0712/82, Imperial College London REC, London, UK). Diagnosis of acute pancreatitis was confirmed by biochemistry +/− imaging. Blood was collected in BD SST Vacutainers, and serum prepared according to manufacturers' instructions, in line with routine clinical practice. The supernatant was stored in aliquots at −80 °C.

Assays on Clinical Serum Samples Using the PLA2GIIA Inhibitor. Phospholipase A2 inhibitor LY 311727 was dissolved in DMSO to prepare the stock solution and then diluted in HEPES (50 mM, pH7). A 5 μL amount of serum was then mixed with 15 μL of HEPES assay buffer containing the appropriate concentration of LY 311727. The solution was left to stand for 10 min before addition of 5 μL of POPG liposome. After a further 10 min, 2 μL of polystreptavidin-coated Au nanoparticles was added and the mixture was introduced to the CN140 test strips. The strips were washed with HEPES assay buffer containing 10 mg/mL BSA.

Amylase Activity. Amylase activity on the clinical samples was determined using the Randox amylase activity assay calibrated against porcine pancreatic amylase. A 4 μL sample of serum was added to 62.5 μL of solution 1 and 12.5 μL of solution 2, and the

rate of absorbance change at 405 nm between 10 and 20 min after substrate addition was measured.

Lipase Activity. Lipase activity was measured using 1,2-di-*O*-lauryl-*rac*-glycero-3-(glutaric acid 6-methylresorufin ester) (DGGR). An assay buffer at pH 8.4 was prepared containing Tris (41 mM), colipase (1 mg/L), sodium deoxycholate (1.8 mM), sodium taurodeoxycholate (7.2 mM), and $CaCl_2$ (0.2 mM), and a substrate buffer was prepared at pH 4.0 containing tartrate (1.6 mM), DGGR (0.2 mM), and $CaCl_2$ (0.2 mM). The assay was performed by mixing 5 μL of serum with 150 μL of assay buffer and 15 μL of substrate buffer. Fluorescence (λ_{ex} = 529 nm, λ_{em} = 600 nm) was measured, and the rate of change between 10 and 20 min after substrate addition was used to generate the reading.

Conflict of Interest: The authors declare the following competing financial interest(s): M.M.S. is an inventor on the patent application WO 2011/113813.

Supporting Information Available: Characterization of PEG linkers and liposomes, lateral flow device (LFD) test of PLA2GIB and PLA2GIIA, inhibition test of human PLA2GIIA, amylase and lipase activity as well as PLA2GIB activity for the pancreatic clinical sera samples, device and control line design experiments, and calculation of detection limit of commercial activity assay kit. This material is available free of charge *via* the Internet at http://pubs.acs.org.

Acknowledgment. The authors acknowledge the Technology Strategy Board (TSB) and the UK Engineering and Physical Sciences Research Council (EPSRC) (EP/K502352/1) and ERC-POC grant Naturale-POC for funding. M.M.S. holds an ERC consolidator grant Naturale-CG. R.C. and Y.L. are thankful to N. Liu for some experimental assistance and D. Aili for useful discussions regarding the assay design.

REFERENCES AND NOTES

1. Cirino, G. Multiple Controls in Inflammation - Extracellular and Intracellular Phospholipase A2, Inducible and Constitutive Cyclooxygenase, and Inducible Nitric Oxide Synthase. *Biochem. Pharmacol.* **1998**, *55*, 105–111.
2. Dennis, E. A. Diversity of Group Types, Regulation, and Function of Phospholipase A2. *J. Biol. Chem.* **1994**, *269*, 13057–13060.
3. Kugiyama, K.; Ota, Y.; Takazoe, K.; Moriyama, Y.; Kawano, H.; Miyao, Y.; Sakamoto, T.; Soejima, H.; Ogawa, H.; Doi, H.; *et al.* Circulating Levels of Secretory Type II Phospholipase A2 Predict Coronary Events in Patients with Coronary Artery Disease. *Circulation* **1999**, *100*, 1280–1284.
4. Eskola, J. U.; Nevalainen, T. J.; Kortesuo, P. Immunoreactive Pancreatic Phospholipase A2 and Catalytically Active Phospholipases A2 in Serum from Patients with Acute Pancreatitis. *Clin. Chem.* **1988**, *34*, 1052–1054.
5. Schrama, A. J. J.; de Beaufort, A. J.; Poorthuis, B. J. H. M.; Berger, H. M.; Walther, F. J. Secretory Phospholipase A2 in Newborn Infants with Sepsis. *J. Perinatol.* **2008**, *28*, 291–296.
6. Menschikowski, M.; Hagelgans, A.; Fuessel, S.; Mareninova, O. A.; Neumeister, V.; Wirth, M. P.; Siegert, G. Serum Levels of Secreted Group Iia Phospholipase A2 in Benign Prostatic Hyperplasia and Prostate Cancer: A Biomarker for Inflammation or Neoplasia? *Inflammation* **2012**, *35*, 1113–1118.
7. Dong, Z.; Liu, Y.; Scott, K. F.; Levin, L.; Gaitonde, K.; Bracken, R. B.; Burke, B.; Zhai, Q. J.; Wang, J.; Oleksowicz, L.; *et al.* Secretory Phospholipase A2-IIa Is Involved in Prostate Cancer Progression and May Potentially Serve as a Biomarker for Prostate Cancer. *Carcinogenesis* **2010**, *31*, 1948–1955.
8. Kupert, E.; Anderson, M.; Liu, Y.; Succop, P.; Levin, L.; Wang, J.; Wikenheiser-brokamp, K.; Chen, P.; Pinney, S. M.; Macdonald, T.; *et al.* Plasma Secretory Phospholipase A2-IIa as a Potential Biomarker for Lung Cancer in Patients with Solitary Pulmonary Nodules. *BMC Cancer* **2011**, *11*, 513–522.
9. Chemburu, S.; Ji, E.; Casana, Y.; Wu, Y.; Buranda, T.; Schanze, K. S.; Lopez, G. P.; Whitten, D. G. Conjugated Polyelectrolyte Supported Bead Based Assays for Phospholipase A2 Activity. *J. Phys. Chem. B* **2008**, *112*, 14492–14499.
10. Feng, L.; Manabe, K.; Shope, J. C.; Widmer, S.; DeWald, D. B.; Prestwich, G. D. A Real-Time Fluorogenic Phospholipase A2 Assay for Biochemical and Cellular Activity Measurements. *Chem. Biol.* **2002**, *9*, 795–803.
11. Okada, S. Y.; Jelinek, R.; Charych, D. Induced Color Change of Conjugated Polymeric Vesicles by Interfacial Catalysis of Phospholipase A2. *Angew. Chem., Int. Ed.* **1999**, *38*, 655–659.
12. Dennis, E. A.; Cao, J.; Hsu, Y.-H.; Magrioti, V.; Kokotos, G. Phospholipase A2 Enzymes: Physical Structure, Biological Function, Disease Implication, Chemical Inhibition, and Therapeutic Intervention. *Chem. Rev.* **2011**, *111*, 6130–6185.
13. Lee, D.-S.; Jeon, B. G.; Ihm, C.; Park, J.-K.; Jung, M. Y. A Simple and Smart Telemedicine Device for Developing Regions: A Pocket-Sized Colorimetric Reader. *Lab Chip* **2011**, *11*, 120–126.
14. Martinez, A. W.; Phillips, S. T.; Carrilho, E.; Thomas, S. W., III; Sindi, H.; Whitesides, G. M. Simple Telemedicine for Developing Regions: Camera Phones and Paper-Based Microfluidic Devices for Real-Time, Off-Site Diagnosis. *Anal. Chem.* **2008**, *80*, 3699–3707.
15. Xiao, Z.; Lie, P.; Fang, Z.; Yu, L.; Chen, J.; Liu, J.; Ge, C.; Zhou, X.; Zeng, L. A Lateral Flow Biosensor for Detection of Single Nucleotide Polymorphism by Circular Strand Displacement Reaction. *Chem. Commun.* **2012**, *48*, 8547–8549.
16. Rohrman, B. A.; Leautaud, V.; Molyneux, E.; Richards-Kortum, R. R. A Lateral Flow Assay for Quantitative Detection of Amplified HIV-1 RNA. *PLoS One* **2012**, *7*, e45611.
17. Xu, H.; Mao, X.; Zeng, Q.; Wang, S.; Kawde, A.-N.; Liu, G. Aptamer-Functionalized Gold Nanoparticles as Probes in a Dry-Reagent Strip Biosensor for Protein Analysis. *Anal. Chem.* **2009**, *81*, 669–675.
18. Liu, G.; Mao, X.; Phillips, J. A.; Xu, H.; Tan, W.; Zeng, L. Aptamer-Nanoparticle Strip Biosensor for Sensitive Detection of Cancer Cells. *Anal. Chem.* **2009**, *81*, 10013–10018.
19. Mazumdar, D.; Liu, J.; Lu, G.; Zhou, J.; Lu, Y. Easy-to-Use Dipstick Tests for Detection of Lead in Paints Using Non-Cross-Linked Gold Nanoparticle-Dnazyme Conjugates. *Chem. Commun.* **2010**, *46*, 1416–1418.
20. Liu, J.; Mazumdar, D.; Lu, Y. A Simple and Sensitive "Dipstick" Test in Serum Based on Lateral Flow Separation of Aptamer-Linked Nanostructures. *Angew. Chem., Int. Ed.* **2006**, *45*, 7955–7959.
21. Saha, K.; Agasti, S. S.; Kim, C.; Li, X.; Rotello, V. M. Gold Nanoparticles in Chemical and Biological Sensing. *Chem. Rev.* **2012**, *112*, 2739–2779.
22. Howes, P. D.; Rana, S.; Stevens, M. M. Plasmonic Nanomaterials for Biodiagnostics. *Chem. Soc. Rev.* **2014**, *43*, 3835–3853.
23. Jans, H.; Huo, Q. Gold Nanoparticle-Enabled Biological and Chemical Detection and Analysis. *Chem. Soc. Rev.* **2012**, *41*, 2849–2866.
24. Jain, P. K.; Lee, K. S.; El-Sayed, I. H.; El-Sayed, M. A. Calculated Absorption and Scattering Properties of Gold Nanoparticles of Different Size, Shape, and Composition: Applications in Biological Imaging and Biomedicine. *J. Phys. Chem. B* **2006**, *110*, 7238–7248.
25. Laromaine, A.; Koh, L.; Murugesan, M.; Ulijn, R. V.; Stevens, M. M. Protease-Triggered Dispersion of Nanoparticle Assemblies. *J. Am. Chem. Soc.* **2007**, *129*, 4156–4157.
26. Elghanian, R.; Storhoff, J. J.; Mucic, R. C.; Letsinger, R. L.; Mirkin, C. A. Selective Colorimetric Detection of Polynucleotides Based on the Distance-Dependent Optical Properties of Gold Nanoparticles. *Science* **1997**, *277*, 1078–1081.
27. Du, J.; Jiang, L.; Shao, Q.; Liu, X.; Marks, R. S.; Ma, J.; Chen, X. Colorimetric Detection of Mercury Ions Based on Plasmonic Nanoparticles. *Small* **2013**, *9*, 1467–1481.
28. Aili, D.; Gryko, P.; Sepulveda, B.; Dick, J. A. G.; Kirby, N.; Heenan, R.; Baltzer, L.; Liedberg, B.; Ryan, M. P.;

Stevens, M. M. Polypeptide Folding-Mediated Tuning of the Optical and Structural Properties of Gold Nanoparticle Assemblies. *Nano Lett.* **2011**, *11*, 5564–5573.
29. Aili, D.; Mager, M.; Roche, D.; Stevens, M. M. Hybrid Nanoparticle-Liposome Detection of Phospholipase Activity. *Nano Lett.* **2011**, *11*, 1401–1405.
30. Mammen, M.; Choi, S. K.; Whitesides, G. M. Polyvalent Interactions in Biological Systems: Implications for Design and Use of Multivalent Ligands and Inhibitors. *Angew. Chem., Int. Ed.* **1998**, *37*, 2755–2794.
31. Lim, Y.-b.; Lee, M. Self-Assembled Multivalent Carbohydrate Ligands. *Org. Biomol. Chem.* **2007**, *5*, 401–405.
32. Huskens, J. Multivalent Interactions at Interfaces. *Curr. Opin. Chem. Biol.* **2006**, *10*, 537–543.
33. Fasting, C.; Schalley, C. A.; Weber, M.; Seitz, O.; Hecht, S.; Koksch, B.; Dernedde, J.; Graf, C.; Knapp, E.-W.; Haag, R. Multivalency as a Chemical Organization and Action Principle. *Angew. Chem., Int. Ed.* **2012**, *51*, 10472–10498.
34. de la Rica, R.; Fratila, R. M.; Szarpak, A.; Huskens, J.; Velders, A. H. Multivalent Nanoparticle Networks as Ultrasensitive Enzyme Sensors. *Angew. Chem., Int. Ed.* **2011**, *50*, 5703–5706.
35. Marsh, D.; Bartucci, R.; Sportelli, L. Lipid Membranes with Grafted Polymers: Physicochemical Aspects. *Biochim. Biophys. Acta, Biomembr.* **2003**, *1615*, 33–59.
36. Li, H. Y.; Park, S. H.; Reif, J. H.; LaBean, T. H.; Yan, H. DNA-Templated Self-Assembly of Protein and Nanoparticle Linear Arrays. *J. Am. Chem. Soc.* **2004**, *126*, 418–419.
37. Chen, C.; Han, D.; Cai, C.; Tang, X. An Overview of Liposome Lyophilization and Its Future Potential. *J. Controlled Release* **2010**, *142*, 299–311.
38. Xu, W.; Yi, L.; Feng, Y.; Chen, L.; Liu, J. Structural Insight into the Activation Mechanism of Human Pancreatic Prophospholipase A2. *J. Biol. Chem.* **2009**, *284*, 16659–16666.
39. Nevalainen, T. J.; Gronroos, J. M.; Kortesuo, P. T. Pancreatic and Synovial Type Phospholipases A2 in Serum Samples from Patients with Severe Acute Pancreatitis. *Gut* **1993**, *34*, 1133–1136.
40. Green, J. A.; Smith, G. M.; Buchta, R.; Lee, R.; Ho, K. Y.; Rajkovic, I. A.; Scott, K. F. Circulating Phospholipase A2 Activity Associated with Sepsis and Septic Shock Is Indistinguishable from That Associated with Rheumatoid Arthritis. *Inflammation* **1991**, *15*, 355–367.
41. Pruzanski, W.; Vadas, P.; Stefanski, E.; Urowitz, M. B. Phospholipase A2 Activity in Sera and Synovial Fluids in Rheumatoid Arthritis and Osteoarthritis. Its Possible Role as a Proinflammatory Enzyme. *J. Rheumatol.* **1985**, *12*, 211–216.
42. Koenig, W.; Vossen, C. Y.; Mallat, Z.; Brenner, H.; Benessiano, J.; Rothenbacher, D. Association between Type II Secretory Phospholipase A2 Plasma Concentrations and Activity and Cardiovascular Events in Patients with Coronary Heart Disease. *Eur. Heart. J.* **2009**, *30*, 2742–2748.
43. Dutour, A.; Achard, V.; Sell, H.; Naour, N.; Collart, F.; Gaborit, B.; Silaghi, A.; Eckel, J.; Alessi, M.-C.; Henegar, C.; *et al.* Secretory Type II Phospholipase A2 Is Produced and Secreted by Epicardial Adipose Tissue and Overexpressed in Patients with Coronary Artery Disease. *J. Clin. Endocrinol. Metab.* **2010**, *95*, 963–967.
44. Schevitz, R. W.; Bach, N. J.; Carlson, D. G.; Chirgadze, N. Y.; Clawson, D. K.; Dillard, R. D.; Draheim, S. E.; Hartley, L. W.; Jones, N. D.; Mihelich, E. D.; *et al.* Structure-Based Design of the First Potent and Selective Inhibitor of Human Non-Pancreatic Secretory Phospholipase A2. *Nat. Struct. Biol.* **1995**, *2*, 458–465.